HHS Public Access

Author manuscript

Dev Biol. Author manuscript; available in PMC 2021 January 01.

Published in final edited form as:

Dev Biol. 2020 January 01; 457(1): 57–68. doi:10.1016/j.ydbio.2019.09.004.

Hyaluronic acid is required for palatal shelf movement and its interaction with the tongue during palatal shelf elevation

Marisa A. Yonemitsu, **Tzu-yin Lin**, **Kai Yu***

Division of Craniofacial Medicine, Department of Pediatrics, University of Washington and Center for Developmental Biology and Regenerative Medicine, Seattle Children's Research Institute, Seattle, WA 98101, USA

Abstract

Palatal shelf elevation is an essential morphogenetic process that results from palatal shelf movement caused by an intrinsic elevating force. The nature of the elevating force remains unclear, but the accumulation of hyaluronic acid (HA) in the extracellular matrix (ECM) of the palatal shelves may play a pivotal role in developing the elevating force. In mammals, HA is synthesized by hyaluronic acid synthases (HAS) that are encoded by three genes (*Has1-3*). Here, we used the *Wnt1-Cre* driver to conditionally disrupt *hyaluronic acid synthase 2* (*Has2*) in cranial neural crest cell lineages. All *Has2* conditional knockout (cko) mice had cleft palate due to failed shelf elevation during palate development. The HA content was significantly reduced in the craniofacial mesenchyme of *Has2* cko mutants. Reduced HA content affected the ECM space and shelf expansion to result in a reduced shelf area and an increased mesenchymal cell density in the palatal shelves of *Has2* cko mutants. We examined palatal shelf movement by removal of the tongue and mandible from unfixed E13.5 and early E14.5 embryonic heads. Reduced shelf expansion in *Has2* cko mutants altered palatal shelf movement in the medial direction resulting in a larger gap between the palatal shelves than that of littermate controls. We further examined palatal shelf movement in the intact oral cavity by culturing explants containing the maxilla, palate, mandible and tongue (MPMT explants). The palatal shelves elevated alongside morphological changes in the tongue after 24-hour culture in MPMT explants of early E14.5 wild type embryos. On the contrary, shelf elevation failed to occur in in MPMT explants of age-matched *Has2* cko mutants because the tongue obstructs palatal shelf movement, suggesting that reduced shelf expansion could be essential for the palatal shelves to interact with the tongue and overcome tongue obstruction during shelf elevation. *Has2* cko mutants also showed micrognathia due to reduced HA content in the mandibular mesenchyme including Meckel's cartilage. Through 3D imaging and morphometric analysis, we demonstrate that mandibular growth results in a significant increase in the vertical dimension of the common oral-nasal cavity that facilitates palatal shelf movement and its interaction with the tongue during shelf elevation.

***Corresponding author**: Kai Yu, M/S C9S-5, 1900 Ninth Avenue, Seattle, WA 98101, kai.yu@seattlechildrens.org, Phone: 206-884-1260, Fax: 206-884-1405.

Competing interests

The authors declare no competing or financial interests.

Keywords

Hyaluronic acid; Secondary palate development; Palatal shelf elevation; Elevating force; Palatal shelf movement; Mandibular growth

Introduction

In mammals, the secondary palate is formed by the fusion of the paired palatal shelves that separate the oral cavity from the nasal cavity. After outgrowth from the maxillary processes, the palatal shelves grow on either side of the tongue and are vertically oriented in the common oral-nasal cavity. For fusion to occur, the palatal shelves must overcome tongue obstruction and elevate from a vertical to a horizontal position, where the medial edge epithelium (MEE) of the opposing shelves approximate for contact and adhesion. Various studies in the past suggest that shelf elevation is achieved through rapid palatal shelf movement (Ferguson, 1978a; Walker and Fraser, 1956). There are two different opinions on how the palatal shelves move during shelf elevation. The rotation model of shelf elevation suggests that shelf elevation could be achieved through a rapid flipping-up movement (Ferguson, 1978a; Lazzaro, 1940; Walker and Ross, 1972; Wee et al., 1979). An alternative model suggests that shelf elevation could be achieved through a remodeling process, in which the palatal shelves protrude from the medial wall and regress at the ventral wall (Walker and Fraser, 1956). Other studies indicate that shelf rotation and remodeling could coexist to control shelf elevation in the anterior and posterior region respectively (Coleman, 1965; Yu and Ornitz, 2011).

Based on the observation of spontaneous palatal shelf movement following tongue removal from freshly dissected unfixed specimens, it has been proposed that shelf elevation results from an elevating force that is present within the palatal shelf itself (Ferguson, 1978a; Walker and Fraser, 1956). The palatal shelves consist of three structural components, epithelial cells, mesenchymal cells and extracellular matrix (ECM) surrounding mesenchymal cells. Hyaluronic acid (HA) is the predominant glycosaminoglycan (GAG) component in the ECM of the palatal shelves, representing about 60% of the total ECM material (Pratt et al., 1973). HA molecules have unique biophysical properties to bind a large amount of water and to enmesh with other extracellular molecules (Comper and Laurent, 1978). The accumulation and hydration of HA in the palatal shelves is thought to generate a physicochemical force, which is also referred to as the turgor force (Ferguson, 1977; Ferguson, 1978b). However, the mechanism of how this turgor force regulates palatal shelf movement during shelf elevation remains controversial.

HA is synthesized by HA synthases on the plasma membrane and is directly released into the extracellular space without going through the Golgi apparatus (Weigel et al., 1997). In mammals, HA synthases are encoded by three different genes (*Has1-3*) that exhibit distinct expression patterns during development (Spicer and McDonald, 1998). Mouse genetic studies suggest that *Has2* is the major source of HA during embryogenesis. Mice lacking of *Has2* die during early embryogenesis, but those lacking *Has1* or *Has3* are viable and exhibit no obvious phenotype (Camenisch et al., 2000). In this study, we conditionally disrupted

Has2 in the cranial neural crest-derived mesenchyme and found that reduced HA content in the craniofacial mesenchyme results in cleft palate and micrognathia. We showed that the HA accumulation in the palatal shelves increases the ECM space to cause shelf expansion, which not only motivates palatal shelf movement but also instigates the interaction between the palatal shelves and tongue during shelf elevation. We discuss the effect of mandibular growth on palate development and suggest that shelf elevation relies on coordinated tissue interactions that occur during orofacial development.

Results

Conditional targeting of *Has2* in the cranial neural crest cell lineages

Previously, Camenisch et al reported that *Has2* null ($Has2^{-/-}$) mice die at E9.5-E10 due to severe cardiac and vascular defects (Camenisch et al., 2000). To overcome the early lethality of *Has2* null mice that prevents assessment of the role of *Has2* in secondary palate development, we conditionally disrupted *Has2* in cranial neural crest-derived mesenchymal tissues by mating *Wnt1-Cre* driver ($Wnt1^{Cre/+}$) with floxed *Has2* ($Has2^{fl/fl}$) mice (Danielian et al., 1998; Liu et al., 2013). *Has2* conditional knockout (cko) ($Wnt1^{Cre/+}$, $Has2^{fl/fl}$) mice died within several hours after birth due to respiratory and feeding difficulties. *Has2* cko mutant mice showed severe orofacial anomalies including micrognathia, tongue protrusion and complete cleft palate (Figure 1A-C). MicroCT scan of the craniofacial skeleton demonstrated that the mandible of *Has2* cko mutant mice was shorter but wider than that of littermate controls (Figure 1D and E). Histological examination revealed that at P0 the palatal shelves of *Has2* cko mutant mice remained lateral to the tongue, which occupied the entire common oral-nasal cavity (Figure 1F).

Reduced HA content in the craniofacial mesenchyme of *Has2* cko mutants

Alcian blue staining is a commonly used method to detect GAGs at the tissue level. In the past, HA distribution in the palatal shelves has been studied by comparing alcian blue staining of hyaluronidase digested histological sections (for non-HA GAGs) with that of undigested adjacent sections (for total GAGs) to indirectly measure the HA content (Brinkley and Morris-Wiman, 1987; Knudsen et al., 1985). We utilized a biotinylated high-affinity HA binding protein (b-HABP) to directly detect HA in the craniofacial tissues on histological sections. At E13.5 when the wedge-shaped palatal shelves have developed, HA was abundantly and uniformly present in the palatal mesenchyme (Figure 2A and B). In *Has2* cko mutants, the HA content was reduced and no longer uniformly present in the palatal mesenchyme (Figure 2C and D). At early E14.5 prior to shelf elevation, the HA content remained uniformly present at a high level in the palatal mesenchyme of littermate controls (Figure 2E and F). In *Has2* cko mutants, the HA content was increased in the anterior palatal mesenchyme when compared with that of E13.5 (Figure 2C and G). In the posterior palatal mesenchyme of *Has2* cko mutants, HA was present in lower levels in the lateral aspect but was almost absent in the medial aspect when compared to that of E13.5 (Figure 2D and H).

In addition to the palatal mesenchyme, HA was also present in other craniofacial regions. At early E14.5, HA was abundant in the maxillary and mandibular mesenchyme including

Meckel's cartilage, but was almost absent in the primordia of the maxilla, palatine bone and mandible where mesenchymal cells has begun to differentiate into osteoblasts through intramembrane ossification (Figure 2I and J). In *Has2* cko mutants, the HA content was significantly reduced in the maxillary and mandibular mesenchyme (Figure 2K and L). HA was only sporadically present in Meckel's cartilage of *Has2* cko mutants (Figure 2L). We found that HA was also weakly present in the tongue mesenchyme and the HA content was not significantly changed in the tongue mesenchyme of *Has2* cko mutants (Figure 2E-H). These results suggest that HAS2 is a major enzyme for producing HA in the craniofacial region especially in the maxillary and mandibular mesenchyme including Meckel's cartilage.

Reduced shelf area in *Has2* cko mutants

To determine how reduced HA content in the craniofacial mesenchyme resulted in cleft palate in *Has2* cko mutants, we used histological analysis to examine shelf morphology during palate development. At E13.5, the palatal shelves were vertically oriented and showed different morphology in the anterior and posterior regions (Figure 3A and B). The palatal shelves in *Has2* cko mutants showed similar differences in shape between the anterior and posterior region but appeared to be small when compared to those of littermate controls (Figure 3C and D). Using a previously described method (Brinkley and Vickerman, 1982), we measured the shelf area on coronal sections (Figure 3A and B). At E13.5 the palatal shelves in *Has2* cko mutants were 24% smaller than those of littermate controls (cko 0.049±0.008 vs wt 0.064±0.01 mm^2, $P<0.05$, n=6 per group) in the anterior region and 23% smaller (cko 0.072±0.006 vs wt 0.093±0.012 mm^2, $P<0.01$, n=6 per group) in the posterior region (Figure 3E). At early E14.5 prior to shelf elevation, the palatal shelves in *Has2* cko mutants remained small when compared to those of littermate controls (Figure 3G-J). Quantitative analysis indicated that at early E14.5 the palatal shelves in *Has2* cko mutants were 20% smaller than those of littermate controls (cko 0.094±0.018 vs wt 0.117±0.026 mm^2, $P<0.05$, n=10 per group) in the anterior region and 13% smaller (cko 0.130±0.010 vs wt 0.150±0.023 mm^2, $P<0.05$, n=10 per group) in the posterior region (Figure 3K). Moreover, we found that at early E14.5 the palatal shelves in *Has2* cko mutants were separated by an apparently widened tongue when compared to that of littermate controls (Figure 3G-J). We measured the distance between the tips of the palatal shelves on coronal sections as previously described (Yu et al., 2015). At E13.5, there was no statistically significant difference in the tip distance between *Has2* cko mutants and littermate controls in both the anterior region (cko 0.715±0.057 vs wt 0.726±0.072 mm, $P>0.05$, n=3 per group) and posterior region (cko 0.701±0.027 vs wt 0.715±0.043 mm, $P>0.05$, n=3 per group) (Figure 3F). At early E14.5, the tip distance in *Has2* cko mutants was 16% wider than that of littermate controls (cko 0.895±0.035 vs wt 0.772±0.070 mm, $P<0.01$, n=5 per group) in the anterior region and 29% wider (cko 0.857±0.046 vs wt 0.662±0.162 mm, $P<0.05$, n=5 per group) in the posterior region (Figure 3L). We further examined shelf morphology at E15.5 when the palatal shelves have elevated and fused during normal development (Figure 3M and N). In *Has2* cko mutants, the palatal shelves were in the vertical position lateral to the tongue at E15.5 (Figure 3O and P). The palatal shelves of *Has2* cko mutants remained vertically oriented at P0 (Figure 1F), suggesting that shelf elevation never occurs during palate development, resulting in cleft palate in *Has2* cko mutants.

Reduced ECM space and increased mesenchymal cell density and in *Has2* cko mutants

Careful histological examination indicated that mesenchymal cells in the palatal shelves of *Has2* cko mutants were densely packed with significantly reduced ECM space between cells when compared to those of littermate controls (Figure 4A-H). We quantitatively analyzed mesenchymal cell density by counting cell nuclei in the entire palatal shelf region shown in shelf area measurement (Figure 3A and B). At E13.5, mesenchymal cell density in the palatal shelves of *Has2* cko mutants was 27% higher than that of littermate controls (cko 18.2±0.2 vs wt 14.3±0.6 nuclei/1000 μm^2, $P<0.001$, n=6 per group) in the anterior region and 11% higher (cko 17.7±0.2 vs wt 15.8±0.1 nuclei/1000 μm^2, $P<0.01$, n=6 per group) in the posterior region (Figure 4I). At early E14.5, mesenchymal cell density in the palatal shelves of *Has2* cko mutants was 21% higher than that of littermate controls (cko 18.3±1.3 vs wt 15.2±0.6 nuclei/1000 μm^2, $P<0.01$, n=6 per group) in the anterior region and 22% higher (cko 20.7±1.6 vs wt 16.9±0.2 nuclei/1000 μm^2, $P<0.01$, n=6 per group) in the posterior region (Figure 4J).

Increased cell density could result from increased cell proliferation during development. We therefore examined cell proliferation through 5-Bromo-2'-deoxyuridine (BrdU) labeling and calculated the BrdU labeling index in the palatal shelves at E13.5 (Figure 5A-D). We found that there was no statistically significant difference in BrdU labeling index between *Has2* cko mutants and littermate controls in both the anterior region (cko 15.5±4.6 vs wt 14.5±4.0 %, $P>0.05$, n=4 per group) and posterior region (cko 29.2±8.9 vs wt 26.1±5.6 %, $P>0.05$, n=4 per group) (Figure 5E). Therefore increased mesenchymal cell density in *Has2* cko mutants more likely results from reduced ECM space than increased cell proliferation, which is consistent with the observation in *Golgb1* mutant embryos that also show reduced HA content in the palatal mesenchyme (Lan et al., 2016). Our results also suggest that the accumulation of HA increases the ECM space to expand the palatal shelves before shelf elevation.

Altered palatal shelf movement in *Has2* cko mutants

To determine if the accumulation of HA is required for generating the intrinsic elevating force, we first examined palatal shelf movement in the absence of the tongue. In a recent in vitro study of shelf elevation, we have shown that removal of the tongue and mandible from fresh dissected unfixed specimens results in rapid shelf movements that reduce the gap between the palatal shelves and causes shelf orientation changes (Yu and Yonemitsu, 2019). We found that the gap between the palatal shelves after ex vivo removal of the tongue and mandible was apparently larger in *Has2* cko mutants than that of age-matched littermate controls (Figure 6A, B, I and J), so we measured the distance between the tips of the palatal shelves on coronal sections. At E13.5, there was no statistically significant difference in the tip distance between *Has2* cko mutants and littermate controls (cko 0.535±0.046 vs wt 0.465±0.079 mm, $P>0.05$, n=4 per group) in the anterior region (Figure 6C, E and G). In the posterior region, the tip distance in *Has2* cko mutants was 34% wider than that of littermate controls (cko 0.511±0.070 vs wt 0.383±0.031 mm, $P<0.05$, n=4 per group) (Figure 6D, F and G). At early E14.5, the tip distance in *Has2* cko mutants was 99% wider than that of littermate controls (cko 0.551±0.060 vs wt 0.276±0.079 mm, $P<0.01$, n=4 per group) in the anterior region (Figure 6K, M and O), and was 82% wider (cko 0.504±0.047 vs wt

0.277±0.035 mm, P<0.001, n=4 per group) in the posterior region (Figure 6L, N and O). We also used a previously described palate shelf index (PSI) to quantify shelf orientation changes (Figure 6C and D) (Wee et al., 1976). The PSI uses values of 1-5 to express the degree of shelf reorientation with the value 1 assigned for a completely vertical shelf and 5 for a completely horizontal shelf. Therefore, the PSI was 1 for the palatal shelves of both *Has2* cko mutants and littermate controls before removal of the tongue and mandible at E13.5 and early E14.5 (Figure 3A-D and G-J). After ex vivo removal of the tongue and mandible at E13.5, the PSI increased to 3.54±0.34 in anterior region and 2.22±0.62 in the posterior region of *Has2* cko mutants (n=8 per group), which was not significantly different from those of littermate controls (3.76±0.37 in the anterior region and 2.50±0.31 in the posterior region, n=8 per group) (Figure 6H). At early E14.5, the PSI increased to 3.39±0.31 in the anterior region of *Has2* cko mutants (n=8 per group), which was not significantly different from that of littermate controls (3.72±0.51, n=8 per group) (Figure 6P). The PSI in the posterior region of *Has2* cko mutants was 15% lower than that of littermate controls (cko 2.93±0.40 vs wt 3.45±0.48, P<0.05, n=8 per group) (Figure 6P), suggesting that shelf reorientation in the posterior region of *Has2* cko mutants was less advanced than that of littermate controls following ex vivo removal of the tongue and mandible (Figure 6L and N).

The large shelf gap in *Has2* cko mutants following ex vivo removal of the tongue and mandible could be caused by an increase of the distance between the tips of the palatal shelves during palate development (Figure 3L). To further test if the HA accumulation is required for palatal shelf movement, we cultured palate explants of E13.5 wild type embryos and used a drug to enhance HA degradation during culture. Norchlorcyclizine (NORCHLR) is the metabolite of chlorcyclizine (CHLR) that can enhance HA degradation without affecting its synthesis and has been shown to induce cleft palate when administered in vivo (Brinkley and Vickerman, 1982; Wilk et al., 1978). Palatal explants were prepared by removal of the tongue, mandible, upper cranial and brain tissues as described previously (Snyder-Warwick et al., 2010), and were cultured with or without NORCHLD for 48 hours. At E13.5, removal of the tongue and mandible left a large gap between the palatal shelves in palatal explants (Figure 7A and B). When cultured without NORCHLD, the palatal shelves made contact in the posterior third and were separated by a small gap in other regions after 24-hour culture (Figure 7C). After 48-hour culture, the palate had closed except in the most anterior and posterior regions in all 10 specimens examined (Figure 7E). When cultured with NORCHLD, the gap between the palatal shelves narrowed after 24-hour culture (Figure 7D) and remained present after 48-hour culture in all 16 specimens examined (Figure 7F). Failure of palatal closure during culture in the presence of NORCHLD suggests that the HA accumulation is essential for the palatal shelves to move in the medial direction.

Failure of shelf elevation in *Has2* cko mutants during MPMT explant culture

During palate development, shelf elevation occurs when the tongue remains present in the common oral-nasal cavity. To further investigate shelf elevation defects in *Has2* cko mutants, we used a newly developed organ culture method to analyze palatal shelf movement in the presence of the tongue and mandible (Yu and Yonemitsu, 2019). We removed the cranium and brain tissues from early E14.5 embryonic heads to generate explants that contained the maxilla, palatal shelves, mandible and tongue (MPMT explants) (Yu and Yonemitsu, 2019).

As the palatal shelves remained vertically oriented, the tongue was retained within the mouth and was not visible prior to culture (Figure 8A, A', B and B'). After 24-hour culture, the tongue protruded out of the slightly opened mouth in all 30 MPMT explants of littermate controls examined (Figure 8C and C'). Removal of the tongue and mandible after culture indicated that the palate had closed except in the most anterior and posterior regions (Figure 8E), or had a small gap between the opposing shelves (Figure 8G and H), which can often be found during normal palate development immediately following shelf elevation (Yu and Ornitz, 2011; Yu and Yonemitsu, 2019). On the contrary, the tongue remained retained within the mouth after 24-hour culture in all 10 MPMT explants of *Has2* cko mutants examined (Figure 8D and D'). Removal of the tongue and mandible after culture indicated that the palatal shelves were separated by a large gap along the entire length of the palate (Figure 8F).

Histological examination indicated that shelf elevation occurred in MPMT explants of littermate controls after 24-hr culture (Figure 8G and H). During the course of shelf elevation, the tongue became flattened in the oral cavity, which is similar to that of in vivo shelf elevation (Yu and Ornitz, 2011). In MPMT explants of *Has2* cko mutants, the palatal shelves remained vertically oriented after 24-hour culture and the tongue continued to occupy the common oral-nasal cavity (Figure 8I and J). It should be noted that the palatal shelves in MPMT explants of *Has2* cko mutants did not show morphological changes that are shown following ex vivo removal of the tongue and mandible (Figure 6M and N), suggesting that failure of shelf elevation in MPMT explants of *Has2* cko mutants is caused by the tongue that obstructs palatal shelf movement during culture.

Meckel's cartilage malformation in *Has2* cko mutants

As shown earlier, the HA content was significantly reduced in mandibular mesenchyme and was almost absent in Meckel's cartilage (Figure 2J and L). Previous studies had shown that HA is essential to chondrogenesis and cartilage formation (Matsumoto et al., 2009; Moffatt et al., 2011; Shibata et al., 2003). We therefore used alcian blue and alizarin red staining to examine Meckel's cartilage formation during mandible development. Meckel's cartilage is formed at E12.5 as two separate rods in the mandibular process (Ramaesh and Bard, 2003). At E13.5, the two rods join at the distal end to form a single V-shaped structure (Figure 9A). In *Has2* cko mutants, Meckel's cartilage was shorter than that of littermate controls and weakly stained by alcian blue (Figure 9B), indicating of reduction of total GAGs in the cartilaginous matrix due to loss of HA (Figure 2L). Mandibular ossification occurs at E14.5 around the time when shelf elevation occurs. At E15.5, the mandible is formed in the mandibular process lateral to Meckel's cartilage. The mandible of *Has2* cko mutants was comparable to that of littermate controls (Figure 9C and D), suggesting that bone formation is not affected by reduced HA content in the mandibular process. However, due to Meckel's cartilage malformation, the mandible of *Has2* cko mutants never reached to the same length as that of littermate controls (Figure 9E and F).

Reduced vertical dimension of the common oral-nasal cavity in *Has2* cko mutants

Mouse genetic studies show that cleft palate often occurs in mice with chondrodysplasia (Donahue et al., 2003; Gaiser et al., 2002; Garofalo et al., 1991; Li et al., 1995; Vandenberg

et al., 1991), suggesting that Meckel's cartilage malformation could also affect palate development in *Has2* cko mutants. It had been hypothesized that mandibular growth could lead to tongue descent that is essential for shelf elevation to occur (Greene and Pratt, 1976). Since mandibular growth, shelf elevation and hypothetical tongue descent occurs along the different anatomical axes during craniofacial development, we combined optical projection tomography (OPT) with a previously developed quantification method to measure the dimensions of the common oral-nasal cavity before shelf elevation (Hart et al., 1969). On virtual sagittal sections rendered from the OPT dataset, we identified four craniofacial landmarks, basion (B), center of the Meckel's cartilage (M), midpoint on the anterior convexity of the nasal septum (N) and center of the hypophysis cerebri (S) to measure the mandibular dimension (MB), the dimension of the posterior cranial base (SB), the horizontal dimension (NB), anterior vertical dimension (N-MB) and posterior vertical dimension (S-MB) of the common oral-nasal cavity (Figure 10A and C). At E13.5, there was no statistically significant difference in the mandibular dimension, the dimension of the posterior cranial base and the dimensions of the common oral-nasal cavity between *Has2* cko mutants and littermate controls (Figure 10A, B and Table 1). At early E14.5, the dimension of the posterior cranial base (SB) in *Has2* cko mutants remained similar to that of littermate controls but the mandibular dimension (MB) in *Has2* cko mutants was 16% smaller than that of littermate controls (Figure 10C, D and Table 1). Moreover, the horizontal dimension (NB), anterior (N-MB) and posterior (S-NB) vertical dimension in *Has2* cko mutants were 8%, 43% and 14% smaller than that of littermate controls respectively (Table 1). Further examination of early E14.5 wild type specimens at different stages of shelf elevation indicated that the tongue and mandible barely changed their position as shelf elevation progressed (Figure 10E-G). On virtual coronal sections rendered from the same OPT dataset, we found that cavity space appeared above the dorsum of the tongue prior to shelf elevation and progressively increased to accommodates the elevated palatal shelf (Figure 10E'-G'). On the contrary, such cavity space did not progressively increase in *Has2* cko mutants when compared with that of littermate controls (Figure 10C' and D'). These results suggest that mandible development does not directly affect the tongue position in the common oral-nasal cavity but could be important for the increase of the vertical dimension of the common oral-nasal cavity and the creation of cavity space during shelf elevation.

Discussion

In this study, we use a mouse genetic approach to target HA synthesis during palate development. Compared with the previous pharmacological approach that uses drugs to enhance HA degradation (Brinkley and Vickerman, 1982; Wilk et al., 1978), our approach provides a better way to analyze palate development in the absence of HA to determine the function of HA. Failure of shelf elevation in *Has2* cko mutants confirms that HA plays an essential role in regulating shelf elevation and therefore allows us to further explore the mechanism of shelf elevation. Interestingly, the HA content is not significantly reduced in the palatal shelves of *Has2* cko mutants. This is probably due to the expression of *Has3*, which overlaps with that of *Has2* in the palatal shelves during development (Galloway et al., 2013; Tien and Spicer, 2005). HAS2 and HAS3 have different enzymatic properties. HAS2

synthesizes very large HA molecules (over 2×10^6 Da), whereas HAS3 synthesizes smaller sizes of HA (2×10^5 to 2×10^6 Da) (Itano and Kimata, 2002). It has been known that the molecular size of HA is essential for HA functions (Cowman et al., 2015; Cyphert et al., 2015; Ruppert et al., 2014; Zgheib et al., 2014). The high molecular weight HA is better at hydrating to form a gel than the low molecular weight forms. Altered shelf morphology in *Has2* cko mutants suggests that loss of *Has2* function cannot be compensated by that of *Has3*, further suggesting that the high molecular weight HA synthesized by HAS2 is indispensable for palatal morphogenesis.

How does HA regulate shelf elevation?

One of the earliest theories suggests that shelf elevation is motivated by a rapid increase in shelf volume due to a considerable increase of intercellular substances in the ECM, especially HA (Brinkley and Vickerman, 1982; Lazzaro, 1940; Pratt et al., 1973; Walker, 1961; Walker and Fraser, 1956). Ferguson postulated that the hydration of HA produces a turgor force to drive palatal shelf movement during shelf elevation (Ferguson, 1978a). The turgor force is defined as the hydrostatic pressure within the cell that pushes the plasma membrane against the cell wall. Therefore, it is not appropriate to use the turgor force to describe physical changes caused by the hydration of HA in the ECM. The hydration of HA increases the ECM space to cause shelf expansion much like air inflating a balloon. Shelf expansion promotes palatal shelf movement in the medial direction that facilitates the subsequent shelf contact and fusion. Interestingly, in the absence of the tongue the palatal shelves of *Has2* cko mutants are capable of changing their orientation to a degree that is comparable to that of littermate controls, suggesting that shelf expansion is not the only motive factor determining shelf elevation. Bulleit and Zimmerman found that removal of the lateral (or presumptive oral) epithelium inhibits shelf reorientation during palate explant culture (Bulleit and Zimmerman, 1985), suggesting that shelf elevation also relies on the palatal epithelium whose development may provide an additional motive factor to promote palatal shelf movement.

During orofacial development, palatal shelf and tongue growth occur concomitantly in the common oral-nasal cavity. Reduced shelf area in *Has2* cko mutants could permit the tongue to occupy more space in the common oral-nasal cavity, therefore increasing the distance between the tips of the palatal shelves. On the other hand, an expanded palatal shelf could compress the tongue and cause tongue morphological changes. Such an interaction between the palatal shelves and tongue could result in the coordinated shelf medial protrusion and tongue flattening during in vivo shelf elevation (Yu and Ornitz, 2011). As MPMT explant culture permits the interaction between the palatal shelves and tongue to occur in vitro (Yu and Yonemitsu, 2019), failure of shelf elevation in MPMT explants of *Has2* cko mutants suggests that HA-mediated shelf expansion not only motivates palatal shelf movement but also instigates the interaction between the palatal shelves and tongue, both of which are essential for shelf elevation to occur.

The role of mandibular growth in palate development

Mandible hypoplasia could affect palate development, which is illustrated in Pierre Robin sequence (PRS), a congenital craniofacial anomaly that is characterized by the triad of micrognathia, glossoptosis and upper airway obstruction as well as a high incident of cleft palate (Cohen, 1999; Evans et al., 2011; Izumi et al., 2012; Robin, 1994). Cleft palate in PRS is often considered as a secondary defect caused by a hypoplastic mandible that leads to shelf elevation defects (Parada et al., 2015). It has been proposed that mandibular growth leads to tongue descent from the common oral-nasal cavity, thereby removing obstruction for shelf elevation to occur. Greene and Pratt suggested that “the forward growth of the mandible presumably carries the base of the tongue from between the shelves posteriorly, and downward growth of the mandible creates room above the tongue anteriorly for the shelves to elevate” (Greene and Pratt, 1976). However, Greene and Pratt also acknowledged that the evidence is inconclusive on whether there is a differential mandibular growth spurt prior to shelf elevation (Greene and Pratt, 1976). Our 3D morphometric analysis of the common oral-nasal cavity also suggests that the tongue may not actually move downward during shelf elevation.

By maintaining the integrity of the oral cavity, MPMT explant culture provides a novel way to study the mechanism of shelf elevation. Although the mandible is an essential component of the MPMT explant, mandibular growth is not required for shelf elevation to occur during MPMT explant culture as we found that shelf elevation can occur when the tip of the mandible is excised prior to culture (data not shown). Therefore, failed shelf elevation in MPMT explants of *Has2* cko mutants during culture is not caused by mandible hypoplasia but instead results from intrinsic shelf defects that affect the interaction between the palatal shelves and tongue as suggested earlier. Interestingly, we found that in vitro shelf elevation does not occur when whole embryonic heads are used for culture (data not shown), but only occurs when the cranium and brain tissues are removed from the embryonic head (as a MPMT explant). Such a requirement suggests that in vivo shelf elevation could involve more complicated morphogenetic processes that cannot be fully recapitulated in vitro. For example, studies of *glutamate decarboxylase 67* (*Gad67*) deficient mice reveals that shelf elevation relies on spontaneous upper jaw movement and mouth opening that are regulated by γ-aminobutyric acid (GABA) mediated neural activity (Iseki et al., 2007; Tsunekawa et al., 2005). Removal of the cranium and brain tissues could reduce resistance to allow movement of the nasomaxillary complex in MPMT explants during culture, resulting in mouth opening that increases the vertical dimension of the common oral-nasal cavity. Our 3D morphometric analysis of the common oral-nasal cavity suggests that mandibular growth can also result in an increased vertical dimension, especially in the anterior region. It is possible that forward mandibular growth supports the tongue to interact with the nasomaxillary complex anteriorly during in vivo palate development. Such an interaction together with spontaneous upper jaw movement causes the nasomaxillary complex to move away from the mandible, which increases the vertical dimension of the common oral-nasal cavity and creates cavity space that facilitates palatal shelf movement and its interaction with the tongue. Therefore, mandibular growth may instigate a series of orofacial tissue interactions during in vivo shelf elevation, which may not be required during MPMT explant

culture. During in vivo shelf elevation, the tongue may not physically move or grow downward following mandibular growth as the tongue-descending hypothesis suggests, but rather may be displaced into the oral cavity through its interaction with the expanding palatal shelves that result from the accumulation and hydration of HA in the ECM of the palatal shelves.

Materials and Methods

Mice

Wnt1-Cre driver (*Wnt1*$^{Cre/+}$) (Danielian et al., 1998) and floxed *Has2* (*Has2*$^{f/f}$) (Liu et al., 2013) mice were maintained on a C57BL/6J genetic background. *Has2* conditional knockout (cko) (*Wnt1*$^{Cre/+}$*; Has2*$^{f/f}$) mice were generated by breeding of *Wnt1*$^{Cre/+}$*; Has2*$^{fl/+}$ compound heterozygous mice with *Has2*$^{f/f}$ homozygous mice. Craniofacial skeletons were examined through alcian blue and alizarin red staining as described previously (Yu et al., 2003). All mouse work was approved by the Animal Care and Use Committee of the Seattle Children's Research Institute.

Histology, histochemistry and immunohistochemistry

Embryos were dissected from the uterus in PBS at a designated post-coitum day (or embryonic day). Embryos were decapitated and the heads were fixed in 4% paraformaldehyde (PFA) overnight at 4°C and embedded in paraffin. Specimens were sectioned coronally (6 μm) and stained with hematoxylin and eosin (H&E) for histological examination.

The HA content in the craniofacial mesenchyme was examined on coronal sections using biotinylated hyaluronic acid binding protein (b-HABP) (EMD Millipore). After deparaffinization and rehydration, sections were digested with 10 μg/ml pepsin in 0.1N HCl for 10 minutes to remove endogenous HABP. After washing in PBS, sections were incubated with b-HABP (1:500 dilution) followed by peroxidase-conjugated streptavidin (ThermoFisher Scientific) and DAB substrate (Vector Labs).

Cell proliferation was determined using BrdU immunohistochemistry. BrdU (5-Bromo-2' deoxyuridine) (Sigma) was injected at 0.1mg/gram body weight 2 hours before specimens were harvested. Anti BrdU mouse monoclonal (BD Biosciences) was used at a 1:200 dilution. Immunohistochemistry was carried out on coronal sections using Histostain-Plus IHC Kit (ThermoFisher Scientific) and DAB Substrate Kit (Vector Labs) according to the manufacturer's instructions. The percentage of BrdU-positive nuclei versus total nuclei in the entire palatal shelves was calculated as the BrdU labeling index.

Histomorphometry

Palatal shelf area was measured using a previously described method (Brinkley and Vickerman, 1982). Briefly, on H&E stained coronal sections, a horizontal line was drawn just on the ventral edge of the nasal septum (anterior region) or the cranial base (posterior region) to intersect the medial border of the palatal shelves. A boundary line (blue lines in Figure 3A and B) that separates the palatal shelf from the maxilla was drawn from the edge

of the oral cavity to the point of intersection of the horizontal line with the nasal shelf surface. The entire palatal region ventral to the boundary line was measured as the shelf area (demarcated by dashed red lines in Figure 3A and B). Mesenchymal cell density in the palatal shelves was calculated by counting cell nuclei in the entire palatal region measured for the shelf area. The distance between the tip of the palatal shelves was measured as described previously (Yu et al., 2015).

Ex vivo induction of palatal shelf movement

On freshly dissected embryonic heads, two incisions at the level of the temporomandibular joint were used to separate the tongue and mandible from the rest of the heads. After separation, the heads were left in PBS for 30 minutes to allow completion of shelf morphological changes and then were fixed with 4% PFA and sectioned for histological examination.

The degree of shelf orientation changes was quantitatively measured using palate shelf index (PSI) that had been described (Wee et al., 1976). Briefly, on H&E stained coronal sections, a horizontal line (dashed red lines in Figure 6C and D) was drawn just at the ventral edge of the nasal septum (anterior) or cranial base (posterior) to represent the horizontal position with the value of 5. A vertical line (solid red lines in Figure 6C and D) perpendicular to the horizontal one was drawn to represent the vertical position with the value of 1. To measure the PSI, a line (blue lines in Figure 6C and D) following the slope of the medial border of the palatal shelves was drawn to cross the vertical line. The acute angle (α) between these two lines was measured and converted into PSI with the formula of {(α /90)*4+1}.

Palate explant culture

Dynamic palate culture was performed as described previously (Snyder-Warwick et al., 2010). Briefly, the palate explant including the palate shelves and the attached maxilla was prepared by removing the tongue, mandible, upper cranial and brain tissues from freshly dissected embryonic heads. Palatal explants were placed in 50-mL conical polypropylene tubes (Falcon) filled with 10 mL of BGJb medium containing L-glutamine (Gibco). Penicillin (50 unit/ml) and streptomycin (50 μg/ml) were added into the culture medium but serum was not added. The culture medium was flushed for three minutes with oxygen and the culture tubes were immediately sealed airtight with size 6 solid rubber stoppers and parafilm to maintain the oxygen concentration in the culture tubes. Palate explants were cultured at 37°C with slow rotation (5 rpm) in a hybridization incubator (Robbins Scientific, Model 400) for 48 hours. Palatal shelf morphology was examined after 24-hour and 48-hour culture.

To enhance HA degradation during culture, norchlorcyclizine (NORCHLR) (Sigma) was dissolved in DMSO and added into the culture medium to a final concentration of 100 μg/ml. In the control group, only DMSO was added into the culture medium. The final concentration of DMSO in the culture medium was 0.1%, which did not affect shelf behaviors during culture by comparing with those without DMSO.

MPMT explant culture

On freshly dissected embryonic heads, an incision just superior to the eye was used to remove the cranium and brain to obtain the orofacial portion of the head that includes the maxilla, palate shelves, mandible and tongue (MPMT explant). The remaining neural tissues on MPMT explants were carefully removed using fine forceps. MPMT explants were placed in a 14-mL round-bottom polypropylene tube (Falcon) filled with 7 mL of BGJb medium containing L-glutamine (Gibco). Penicillin (50 unit/ml) and streptomycin (50 μg/ml) were added into the culture medium but serum was not added. The culture medium was flushed for three minutes with oxygen followed by three seconds with carbon dioxide. The oxygen concentration in the culture tubes was not maintained by leaving the culture tubes in air for several minutes before capping them with supplied caps. MPMT explants were cultured at 37°C with slow rotation (5 rpm) in a hybridization incubator (Robbins Scientific, Model 400). As the culture tubes were placed on the rotator in a slightly tilted position, the culture medium would be gently rocked twice on each turn of rotation. After 24-hour culture, MPMT explants were fixed with 4% PFA for shelf morphological examination either through sectioning or by removal of the tongue and mandible from MPMT explants.

Optical tomography and micro-computed tomography

Optical projection tomography (OPT) and micro-computed tomography (microCT) were conducted in the Small ANimal Tomographic Analysis (SANTA) Facility at the Seattle Children's Research Institute. Samples for OPT were prepared and imaged under UV light using a Bioptonics 3001M scanner as described previously (Zovein et al., 2010). MicroCT imaging was performed using a model 1076 in vivo scanner (Skyscan, Belgium). Standard settings were used for imaging of the craniofacial bones (Vora et al., 2016). Raw OPT and microCT scan data were reconstructed using NRecon V1.6.9.4 software (Skyscan, Belgium) and imported into the Drishti Volume Exploration software V 2.6.1 or 3D Slicer (open source visualization software) for 3D rendering and image capture. Virtual sagittal or coronal cut was made using 3D Slicer to generate virtual sagittal or coronal sections from 3D-rendered OPT scans of embryonic heads.

Landmark-based morphometric analysis

The dimensions of the common oral-nasal cavity were measured using previously described method (Hart et al., 1969). Briefly, four landmarks, basion (B), center of the Meckel's cartilage (M), midpoint on the anterior convexity of the nasal septum (N) and center of the hypophysis cerebri (S), were identified on virtual sagittal sections generated from 3D-rendered OPT scans of embryonic heads (red dots in Figure 10A and C). The linear distances between S and B (SB), M and B (MB), and N and B (NB) (solid red lines in Figure 10A and C) were measured for the dimension of the posterior cranial base, mandible dimension and horizontal dimension of the common oral-nasal cavity respectively. The anterior and posterior vertical dimensions of the common oral-nasal cavity were determined by measuring the vertical distance between N and MB extension (N-MB) and between S and the MB (S-MB) (solid yellow lines in Figure 10A and C) respectively.

Statistics

The data were reported as Mean ± Standard deviation (SD) and were analyzed using a two-tailed Student's *t*-test. Changes with P value less than 0.05 were considered to be statistically significant. At least three specimens per group were used in each experiment.

Acknowledgements

We thank Dr. Chin Chiang of Vanderbilt University for providing floxed *Has2* mice and thank Dr. Michael Cunningham for critical reading of the manuscript. This work was supported by NIH grant DE025077 (KY) and by the Seattle Children's Craniofacial Center.

Grant support information:

NIH grant DE025077

References

Brinkley LL, Morris-Wiman J, 1987 Computer-assisted analysis of hyaluronate distribution during morphogenesis of the mouse secondary palate. Development. 100, 629–35. [PubMed: 3443049]

Brinkley LL, Vickerman MM, 1982 The effects of chlorcyclizine-induced alterations of glycosaminoglycans on mouse palatal shelf elevation in vivo and in vitro. Journal of Embryology and Experimental Morphology. 69, 193–213. [PubMed: 6126516]

Bulleit RF, Zimmerman EF, 1985 The influence of the epithelium on palate shelf reorientation. Journal of Embryology and Experimental Morphology. 88, 265–79. [PubMed: 3935750]

Camenisch TD, et al., 2000 Disruption of hyaluronan synthase-2 abrogates normal cardiac morphogenesis and hyaluronan-mediated transformation of epithelium to mesenchyme. J Clin Invest. 106, 349–60. [PubMed: 10930438]

Cohen MM Jr., 1999 Robin sequences and complexes: causal heterogeneity and pathogenetic/phenotypic variability. Am J Med Genet. 84, 311–5. [PubMed: 10340643]

Coleman RD, 1965 DEVELOPMENT OF THE RAT PALATE. Anatomical Record. 151, 107–17. [PubMed: 14278705]

Comper WD, Laurent TC, 1978 Physiological function of connective tissue polysaccharides. Physiol Rev. 58, 255–315. [PubMed: 414242]

Cowman MK, et al., 2015 The Content and Size of Hyaluronan in Biological Fluids and Tissues. Front Immunol. 6, 261. [PubMed: 26082778]

Cyphert JM, et al., 2015 Size Matters: Molecular Weight Specificity of Hyaluronan Effects in Cell Biology. Int J Cell Biol. 2015, 563818. [PubMed: 26448754]

Danielian PS, et al., 1998 Modification of gene activity in mouse embryos in utero by a tamoxifen-inducible form of Cre recombinase. Curr. Biol 8, 1323–6. [PubMed: 9843687]

Donahue LR, et al., 2003 A missense mutation in the mouse Col2a1 gene causes spondyloepiphyseal dysplasia congenita, hearing loss, and retinoschisis. J Bone Miner Res. 18, 1612–21. [PubMed: 12968670]

Evans KN, et al., 2011 Robin sequence: from diagnosis to development of an effective management plan. Pediatrics. 127, 936–48. [PubMed: 21464188]

Ferguson MW, 1977 The mechanism of palatal shelf elevation and the pathogenesis of cleft palate. Virchows Archiv. A. Pathological Anatomy and Histology. 375, 97–113. [PubMed: 143115]

Ferguson MW, 1978a Palatal shelf elevation in the Wistar rat fetus. Journal of Anatomy. 125, 555–77. [PubMed: 640958]

Ferguson MW, 1978b The teratogenic effects of 5-fluoro-2-desoxyuridine (F.U.D.R.) on the Wistar rat fetus with particular reference to cleft palate. J Anat. 126, 37–49. [PubMed: 148445]

Gaiser KG, et al., 2002 Y-position collagen II mutation disrupts cartilage formation and skeletal development in a transgenic mouse model of spondyloepiphyseal dysplasia. J Bone Miner Res. 17, 39–47. [PubMed: 11771668]

Galloway JL, et al., 2013 The control and importance of hyaluronan synthase expression in palatogenesis. Front Physiol. 4, 10. [PubMed: 23382716]

Garofalo S, et al., 1991 Reduced amounts of cartilage collagen fibrils and growth plate anomalies in transgenic mice harboring a glycine-to-cysteine mutation in the mouse type II procollagen alpha 1-chain gene. Proc Natl Acad Sci U S A. 88, 9648–52. [PubMed: 1946380]

Greene RM, Pratt RM, 1976 Developmental aspects of secondary palate formation. Journal of Embryology and Experimental Morphology. 36, 225–45. [PubMed: 1033980]

Hart JC, et al., 1969 Sagittal growth of the craniofacial complex in normal embryonic mice. Arch Oral Biol. 14, 995–7. [PubMed: 5257846]

Iseki S, et al., 2007 Experimental induction of palate shelf elevation in glutamate decarboxylase 67-deficient mice with cleft palate due to vertically oriented palatal shelf. Birth Defects Res A Clin Mol Teratol. 79, 688–95. [PubMed: 17849453]

Itano N, Kimata K, 2002 Mammalian hyaluronan synthases. IUBMB Life. 54, 195–9. [PubMed: 12512858]

Izumi K, et al., 2012 Underlying genetic diagnosis of Pierre Robin sequence: retrospective chart review at two children's hospitals and a systematic literature review. J Pediatr. 160, 645–650 e2. [PubMed: 22048048]

Knudsen TB, et al., 1985 Histochemical localization of glycosaminoglycans during morphogenesis of the secondary palate in mice. Anatomy and Embryology. 173, 137–42. [PubMed: 2416245]

Lan Y, et al., 2016 Golgb1 regulates protein glycosylation and is crucial for mammalian palate development. Development. 143, 2344–55. [PubMed: 27226319]

Lazzaro C, 1940 Sul meccanismo di chiusura del palato secondario. Monitore zoologico italiano. 51, 249–273.

Li SW, et al., 1995 Transgenic mice with targeted inactivation of the Col2 alpha 1 gene for collagen II develop a skeleton with membranous and periosteal bone but no endochondral bone. Genes Dev. 9, 2821–30. [PubMed: 7590256]

Liu J, et al., 2013 Sonic hedgehog signaling directly targets Hyaluronic Acid Synthase 2, an essential regulator of phalangeal joint patterning. Dev Biol. 375, 160–71. [PubMed: 23313125]

Matsumoto K, et al., 2009 Conditional inactivation of Has2 reveals a crucial role for hyaluronan in skeletal growth, patterning, chondrocyte maturation and joint formation in the developing limb. Development. 136, 2825–35. [PubMed: 19633173]

Moffatt P, et al., 2011 Hyaluronan production by means of Has2 gene expression in chondrocytes is essential for long bone development. Dev Dyn. 240, 404–12. [PubMed: 21246657]

Parada C, et al., 2015 Disruption of the ERK/MAPK pathway in neural crest cells as a potential cause of Pierre Robin sequence. Development. 142, 3734–45. [PubMed: 26395480]

Pratt RM, et al., 1973 Acid mucopolysaccharide synthesis in the secondary palate of the developing rat at the time of rotation and fusion. Developmental Biology. 32, 230–7. [PubMed: 4275096]

Ramaesh T, Bard JB, 2003 The growth and morphogenesis of the early mouse mandible: a quantitative analysis. J Anat. 203, 213–22. [PubMed: 12924821]

Robin P, 1994 A fall of the base of the tongue considered as a new cause of nasopharyngeal respiratory impairment: Pierre Robin sequence, a translation. 1923. Plast Reconstr Surg. 93, 1301–3. [PubMed: 8171154]

Ruppert SM, et al., 2014 Tissue integrity signals communicated by high-molecular weight hyaluronan and the resolution of inflammation. Immunol Res. 58, 186–92. [PubMed: 24614953]

Shibata S, et al., 2003 In situ hybridization and immunohistochemistry of versican, aggrecan and link protein, and histochemistry of hyaluronan in the developing mouse limb bud cartilage. J Anat. 203, 425–32. [PubMed: 14620382]

Snyder-Warwick AK, et al., 2010 Analysis of a gain-of-function FGFR2 Crouzon mutation provides evidence of loss of function activity in the etiology of cleft palate. Proc Natl Acad Sci U S A. 107, 2515–20. [PubMed: 20133659]

Spicer AP, McDonald JA, 1998 Characterization and molecular evolution of a vertebrate hyaluronan synthase gene family. J Biol Chem. 273, 1923–32. [PubMed: 9442026]

Tien JY, Spicer AP, 2005 Three vertebrate hyaluronan synthases are expressed during mouse development in distinct spatial and temporal patterns. Developmental Dynamics. 233, 130–41. [PubMed: 15765504]

Tsunekawa N, et al., 2005 Development of spontaneous mouth/tongue movement and related neural activity, and their repression in fetal mice lacking glutamate decarboxylase 67. European Journal of Neuroscience. 21, 173–8. [PubMed: 15654854]

Vandenberg P, et al., 1991 Expression of a partially deleted gene of human type II procollagen (COL2A1) in transgenic mice produces a chondrodysplasia. Proc Natl Acad Sci U S A. 88, 7640–4. [PubMed: 1881905]

Vora SR, et al., 2016 Postnatal Ontogeny of the Cranial Base and Craniofacial Skeleton in Male C57BL/6J Mice: A Reference Standard for Quantitative Analysis. Front Physiol. 6, 417. [PubMed: 26793119]

Walker BE, 1961 The association of mucopolysaccharides with morphogenesis of the palate and other structures in mouse embryos. J Embryol Exp Morphol. 9, 22–31. [PubMed: 13782695]

Walker BE, Fraser FC, 1956 Closure of the Secondary Palate in Three Strains of Mice. J Embryol Exp Morphol. 4, 176–189.

Walker BE, Ross LM, 1972 Observation of palatine shelves in living rabbit embryos. Teratology. 5, 97–101. [PubMed: 5014453]

Wee EL, et al., 1979 Palate morphogenesis. IV. Effects of serotonin and its antagonists on rotation in embryo culture. J Embryol Exp Morphol. 53, 75–90. [PubMed: 536697]

Wee EL, et al., 1976 Palate shelf movement in mouse embryo culture: evidence for skeletal and smooth muscle contractility. Dev Biol. 48, 97–103. [PubMed: 1245264]

Weigel PH, et al., 1997 Hyaluronan synthases. J Biol Chem. 272, 13997–4000. [PubMed: 9206724]

Wilk AL, et al., 1978 Chlorcyclizine induction of cleft palate in the rat: degradation of palatal glycosaminoglycans. Teratology. 18, 199–209. [PubMed: 31013]

Yu K, et al., 2015 Mesenchymal fibroblast growth factor receptor signaling regulates palatal shelf elevation during secondary palate formation. Dev Dyn. 244, 1427–38. [PubMed: 26250517]

Yu K, Ornitz DM, 2011 Histomorphological study of palatal shelf elevation during murine secondary palate formation. Dev. Dyn 240, 1737–1744. [PubMed: 21618642]

Yu K, et al., 2003 Conditional inactivation of FGF receptor 2 reveals an essential role for FGF signaling in the regulation of osteoblast function and bone growth. Development. 130, 3063–74. [PubMed: 12756187]

Yu K, Yonemitsu MA, 2019 In Vitro Analysis of Palatal Shelf Elevation During Secondary Palate Formation. Anat Rec (Hoboken). 302, 1594–1604. [PubMed: 30730607]

Zgheib C, et al., 2014 Targeting Inflammatory Cytokines and Extracellular Matrix Composition to Promote Wound Regeneration. Adv Wound Care (New Rochelle). 3, 344–355. [PubMed: 24757589]

Zovein AC, et al., 2010 Vascular remodeling of the vitelline artery initiates extravascular emergence of hematopoietic clusters. Blood. 116, 3435–44. [PubMed: 20699440]

Highlights

- Reduced mesenchymal HA content results in cleft palate and micrognathia
- The HA accumulation promotes palatal shelf expansion and movement
- Palatal shelf elevation relies on the palatal shelf-tongue interaction
- Mandibular growth regulates the vertical dimension of the oral-nasal cavity

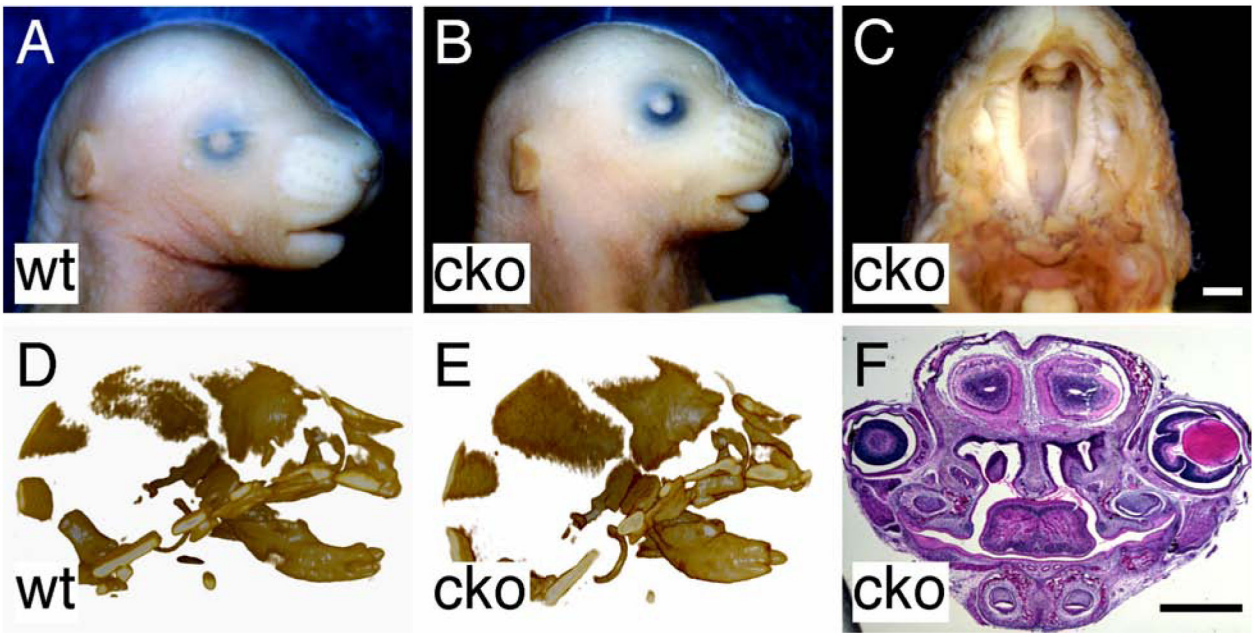

Figure 1.

Craniofacial anomalies in mice lacking *Has2* in cranial neural crest cell lineages. (A) Gross appearance of the head of a P0 wild type mouse. (B) Gross appearance of the head of a P0 *Has2* cko mouse. (C) Inferior view of cleft palate in a P0 *Has2* cko mouse. (D) Lateral view of the 3D rendered craniofacial skeleton from microCT scan of a P0 wild type mouse head. (E) Lateral view of the 3D rendered craniofacial skeleton from microCT scan of a P0 *Has2* cko mouse head. (F) Histological examination of palatal shelf morphology in a P0 *Has2* cko mouse. Scale bars: 1mm.

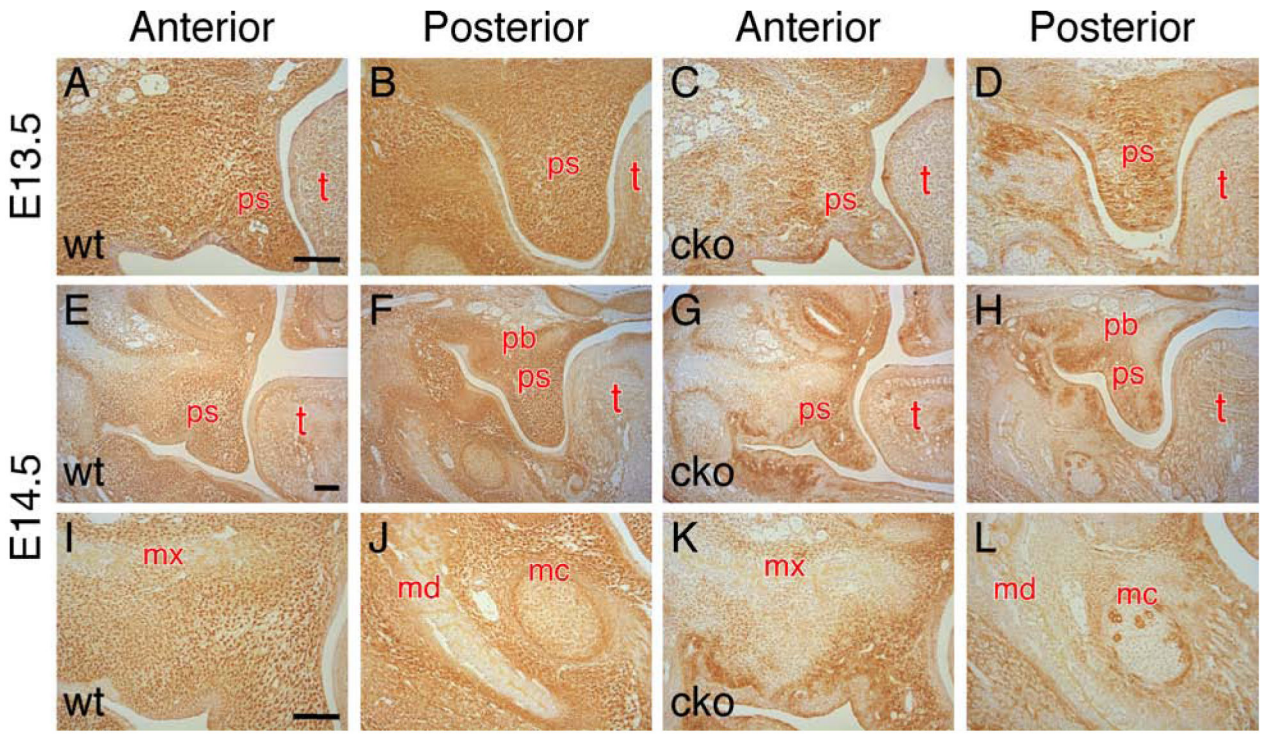

Figure 2.

Has2 cko mutants exhibit reduced HA content in the craniofacial mesenchyme. (A-D) Histochemistry using biotinylated HABP to examine the HA content on serial coronal sections of E13.5 wild type (A and B) and *Has2* cko (C and D) embryonic heads. (E-H) Histochemistry using biotinylated HABP to examine the HA content on serial coronal sections of early E14.5 wild type (E and F) and *Has2* cko (G and H) embryonic heads. (I and J) Magnified view of the HA content in the maxillary (I) and mandibular (J) mesenchyme of an early E14.5 wild type embryo. (K and L) Magnified view of the HA content in the maxillary (K) and mandibular (L) mesenchyme of an early E14.5 *Has2* cko embryo. md, mandible; mc, Meckel's cartilage; mx, maxilla; pb, palatine bone; ps, palatal shelf; t, tongue. Scale bars, 100μm.

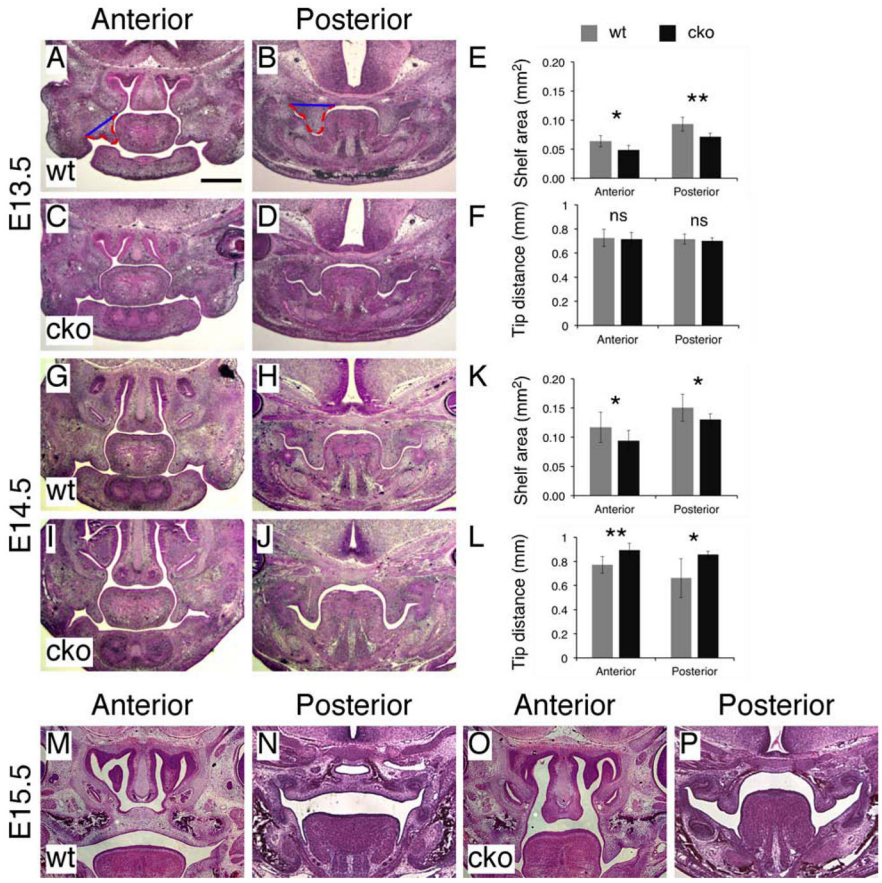

Figure 3.

Has2 cko mutants exhibit reduced shelf area and failure of shelf elevation. (A-D) Histological examination of palatal shelf morphology in E13.5 wild type (A and B) and *Has2* cko (C and D) embryos. Blue lines in A and B separating the palatal shelf from the maxilla and dashed red lines demarcating the edge of the palatal shelves for shelf area measurement. (E) Shelf area measurements in E13.5 wild type and *Has2* cko embryos. (F) Measurements of the distance between the tips of the palatal shelves in E13.5 wild type and *Has2* cko embryos. (G-J) Histological examination of palatal shelf morphology in early E14.5 wild type (G and H) and *Has2* cko (I and J) embryos. (K) Shelf area measurements in early E14.5 wild type and *Has2* cko embryos. (L) Measurements of the distance between the tips of the palatal shelves in early E14.5 wild type and *Has2* cko embryos. (M-P) Histological examination of palatal shelf morphology in E15.5 wild type (M and N) and *Has2* cko (O and P) embryos. *, P value<0.05; **, P value<0.01. Scale bar: 500μm.

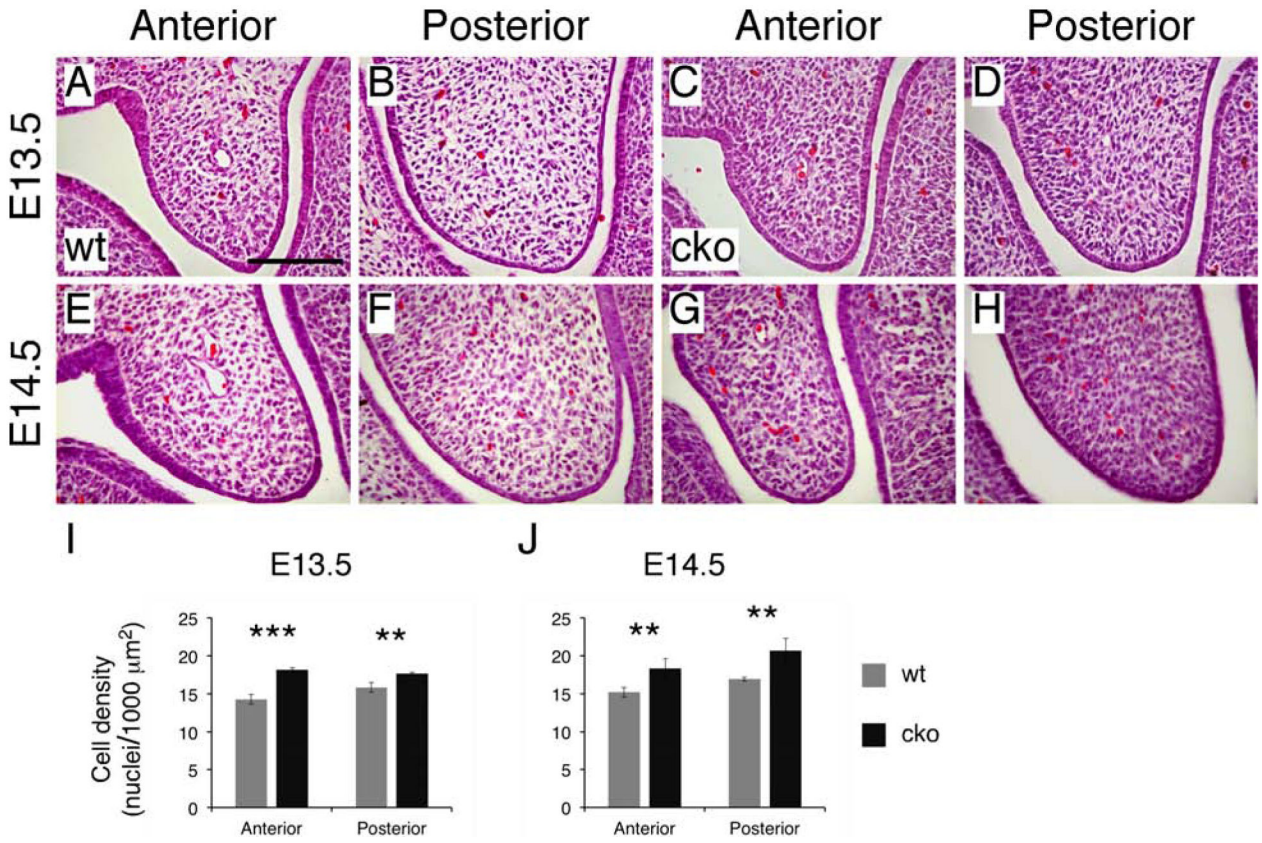

Figure 4.

Has2 cko mutants exhibit reduced mesenchyme cell density in the palatal shelves. (A-D) Magnified view of cell morphology at the tip of the palatal shelves in E13.5 wild type (A and B) and *Has2* cko (C and D) embryos. (E-H) Magnified view of cell morphology at the tip of the palatal shelves in early E14.5 wild type (E and F) and *Has2* cko (G and H) embryos. (I) Quantification of mesenchymal cell density in the entire palatal shelves of E13.5 wild type and *Has2* cko embryos. (J) Quantification of mesenchymal cell density in the entire palatal shelves of early E14.5 wild type and *Has2* cko embryos. **, P value<0.01; ***, P value<0.001. Scale bar: 100μm.

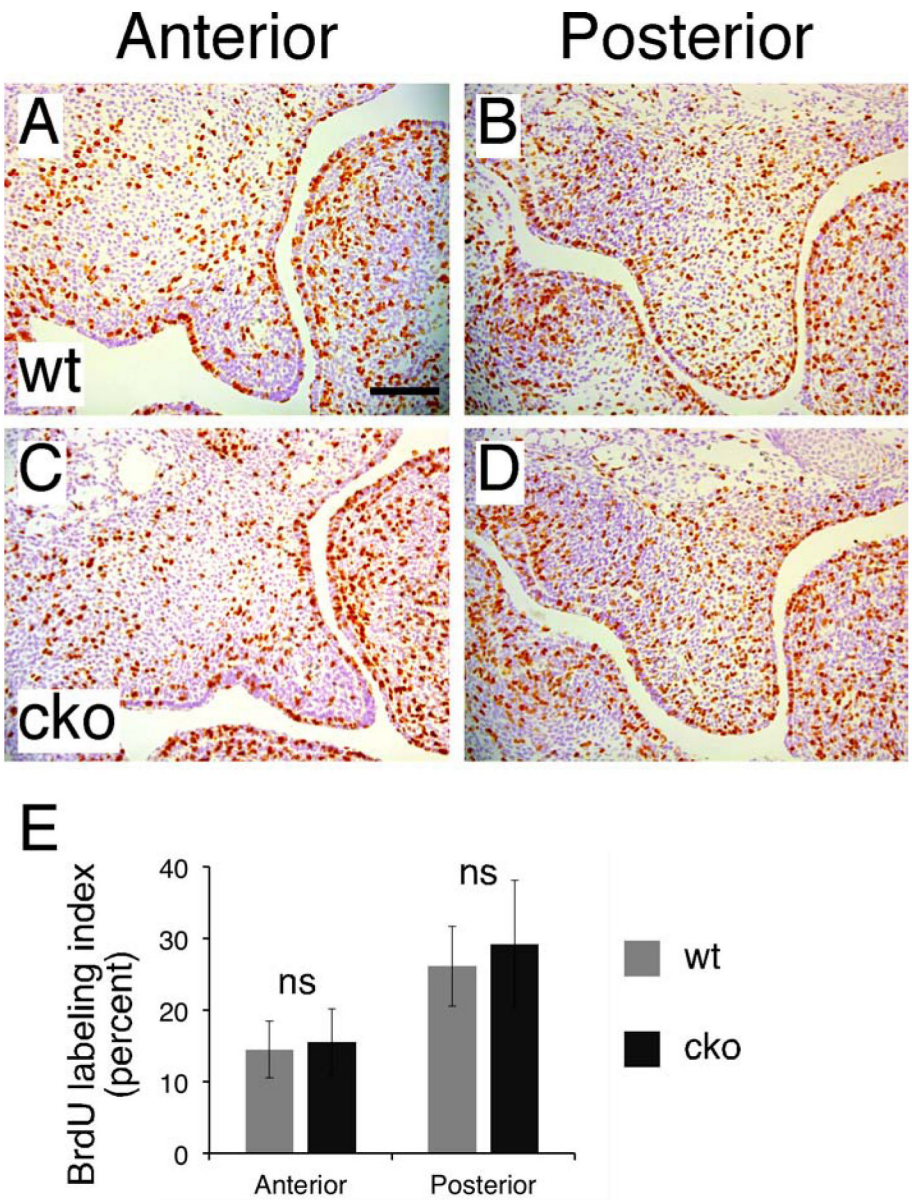

Figure 5.

Analysis of mesenchymal cell proliferation in the palatal shelves. (A-D) BrdU immunohistochemistry to examine mesenchymal cell proliferation in the palatal shelves of E13.5 wild type (A and B) and *Has2* cko (C and D) embryos. (E) Quantification of BrdU labeled mesenchymal cells in the entire palatal shelves of E13.5 wild type and *Has2* cko embryos. ns, not significant. Scale bar: 100μm.

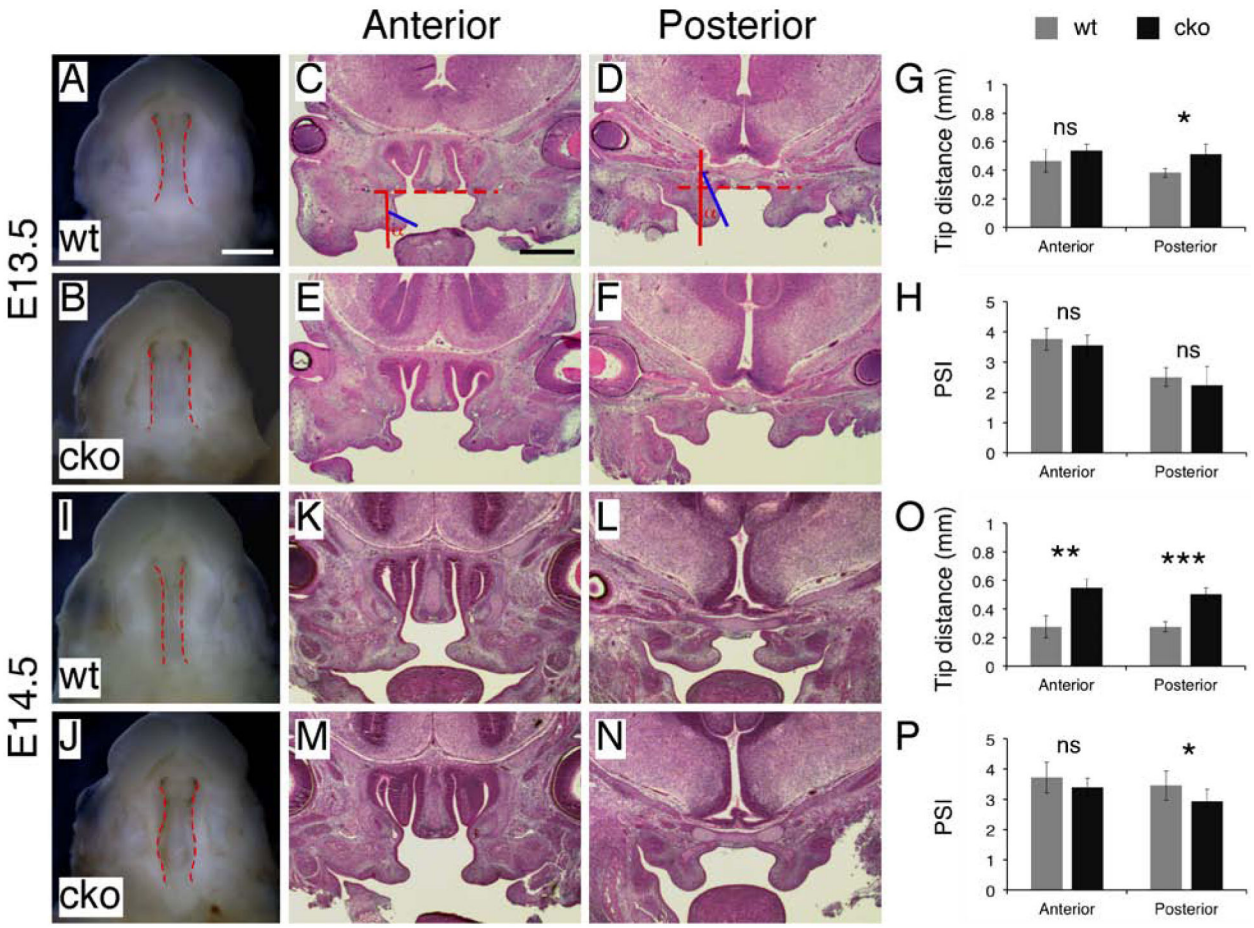

Figure 6.

Analysis of palatal shelf movement following ex vivo removal of the tongue and mandible. (A and B) Inferior view of the gap between the palatal shelves following ex vivo induction of palatal shelf movement in E13.5 wild type (A) and *Has2* cko (B) embryos. Dashed red lines demarcating the medial edges of the palatal shelves. (C-F) Histological examination of palatal shelf morphology following ex vivo induction of palatal shelf movement in E13.5 wild type (C and D) and *Has2* cko (E and F) embryos. The dashed and solid red lines in C and D marking the horizontal and vertical positions in the common oral-nasal cavity respectively. The angle (α) between the solid red and blue line used for calculating the PSI. (G) Measurements of the distance between the tips of the palatal shelves following ex vivo induction of palatal shelf movement in E13.5 wild type and *Has2* cko embryos. (H) PSI in E13.5 wild type and *Has2* cko embryos following ex vivo induction of palatal shelf movement. (I and J) Inferior view of the gap between the palatal shelves following ex vivo induction of palatal shelf movement in early E14.5 wild type (I) and *Has2* cko (J) embryos. Dashed red lines demarcating the medial edges of the palatal shelves. (K-N) Histological examination of palatal shelf morphology following ex vivo induction of palatal shelf movement in early E14.5 wild type (K and L) and *Has2* cko (M and N) embryos. (O) Measurements of the distance between the tips of the palatal shelves following ex vivo induction of palatal shelf movement in early E14.5 wild type and *Has2* cko embryos. (P) PSI in early E14.5 wild type and *Has2* cko embryos following ex vivo induction of palatal shelf

movement. *, P value<0.05; **, P value<0.01; ***, P value<0.001; ns, not significant. Scale bar in A: 1mm; in C: 500μm.

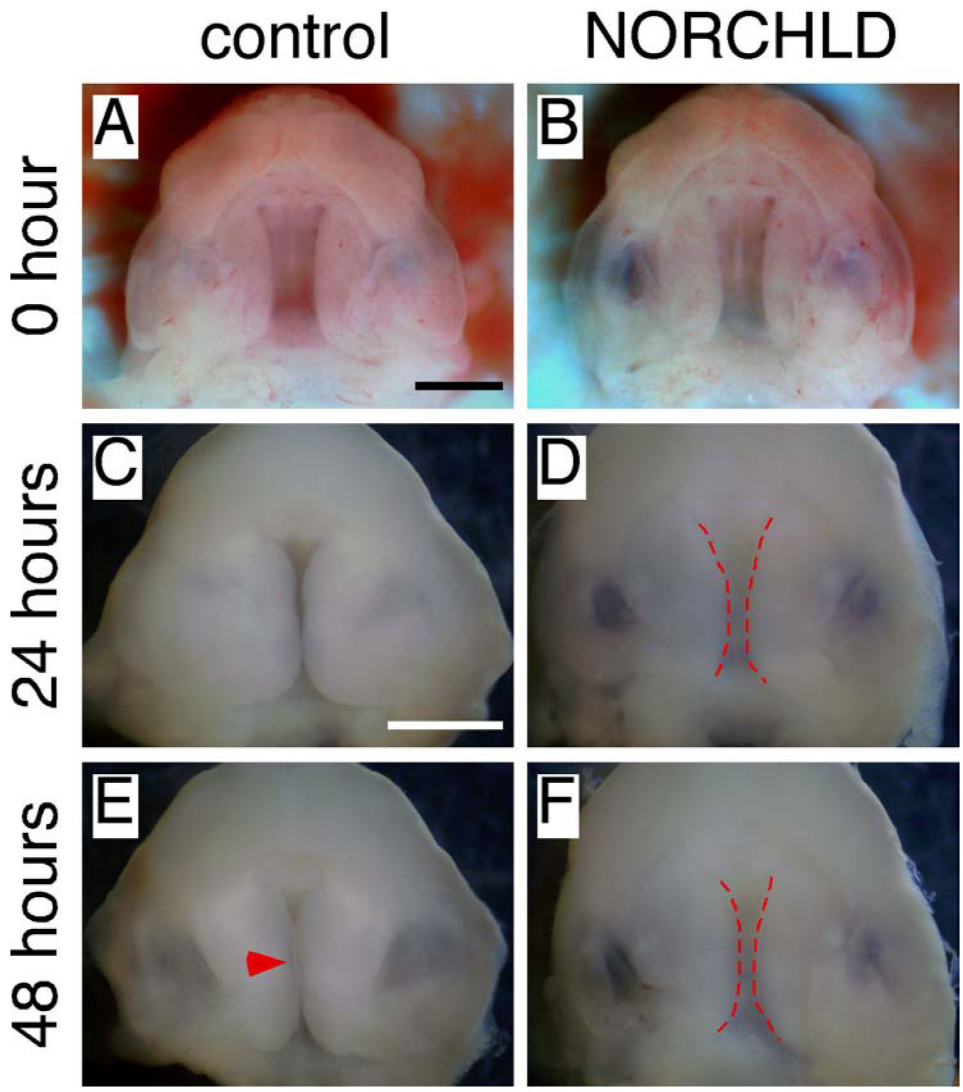

Figure 7.

Enhanced HA degradation prevents palate closure during palate explant culture. (A and B) Inferior view of the palatal shelves and gap between the palatal shelves in wild type E13.5 palate explants before culture. (C and D) Inferior view of the palatal shelves and gap between the palatal shelves in wild type E13.5 palate explants after 24-hour culture. (E and F) Inferior view of the palatal shelves and gap between the palatal shelves in wild type E13.5 palate explants after 48-hour culture. NORCHLD is used to enhance HA degradation during culture in B, D and F. Arrowhead indicating the closed palate. Dashed red lines demarcating the medial edges of the palatal shelves. Scale bars: 1 mm.

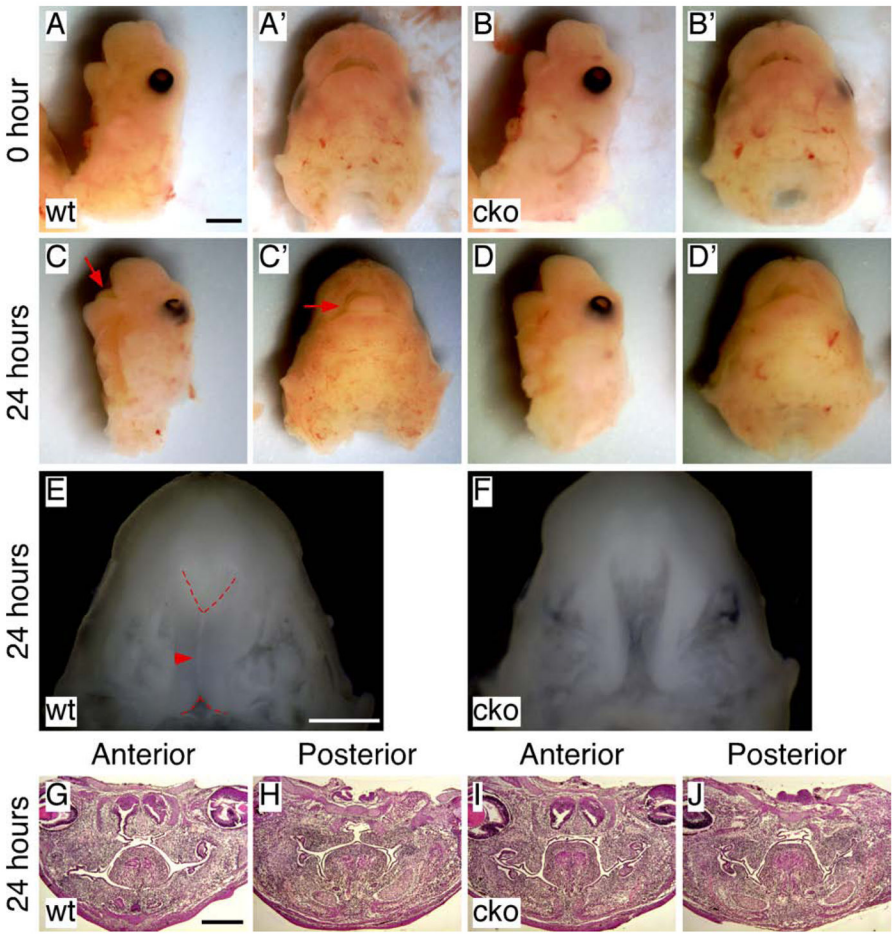

Figure 8.

Analysis of palatal shelf elevation using MPMT explant culture. (A and B) Lateral view of early E14.5 wild type (A) and *Has2* cko (B) MPMT explants before culture. (A' and B') Inferior view of the MPMT explants shown in A and B. (C and D) Lateral view of early E14.5 wild type (C) and *Has2* cko (D) MPMT explants shown in A and B after 24-hour culture. (C' and D') Inferior view of cultured MPMT explants shown in C and D. Arrows indicating the protruded tongue. (E and F) Inferior view of the palatal shelves and gap between the palatal shelves after 24-hour culture in wild type (E) and *Has2* cko (F) MPMT explants by removing the tongue and mandible. Arrowhead indicating the closed palate. Dashed red lines demarcating the medial edges of the palatal shelves. (G and H) Histological examination of palatal shelf morphology in cultured wild type MPMT explants shown in C. (I and J) Histological examination of palatal shelf morphology in cultured *Has2* cko MPMT explants shown in D. Scale bars in A and E: 1mm; in E: 500μm.

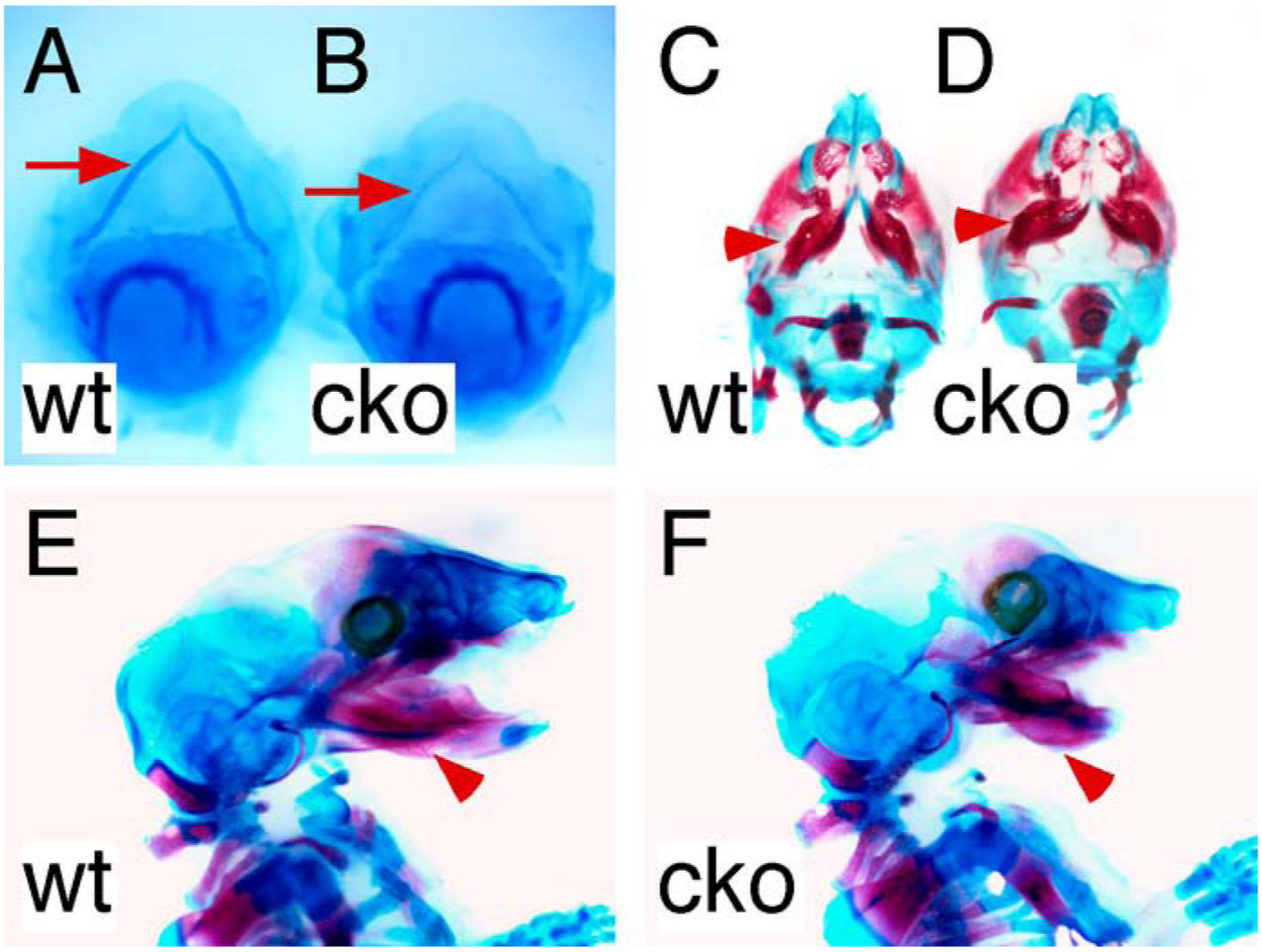

Figure 9.

Meckel's cartilage malformation in *Has2* cko mutants. (A and B) Alcian blue and alizarin red stained craniofacial skeletons of E13.5 wild type (A) and *Has2* cko (B) embryos. (C and D) Alcian blue and alizarin red stained craniofacial skeletons of E15.5 wild type (C) and *Has2* cko (D) embryos. (E and F) Alcian blue and alizarin red stained craniofacial skeletons of E18.5 wild type (E) and *Has2* cko (F) embryos. Arrows indicating Meckel's cartilage. Arrowheads indicating the mandible.

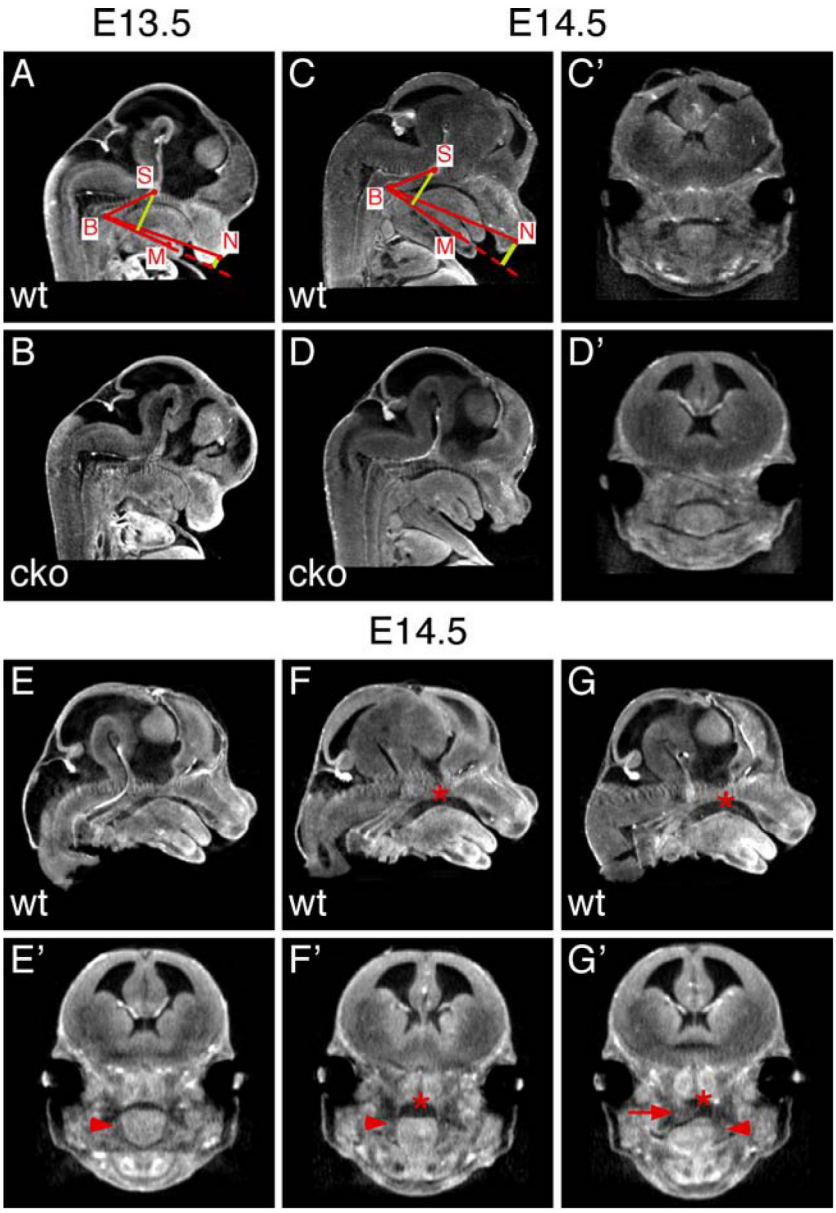

Figure 10.

Morphometric analysis of the dimensions of the common oral-nasal cavity. (A and B) Virtual mid-sagittal sections generated from 3D-rendered OPT scans of E13.5 wild type (A) and *Has2* cko (B) embryonic heads. (C and D) Virtual mid-sagittal sections generated from 3D-rendered OPT scans of early E14.5 wild type (C) and *Has2* cko (D) embryonic heads. Red dots in A and C marking the landmarks for drawing solid red and yellow lines and measuring the dimensions of the common oral-nasal cavity. (C' and D') Virtual coronal sections in the middle region of the palatal shelves generated from the same 3D-rendered OPT scans shown in C and D. (E-G) Virtual mid-sagittal sections generated from 3D-rendered OPT scans of early E14.5 wild type embryos from a same litter. (E'-G') Virtual coronal sections in the middle region of the palatal shelves generated from the same 3D-

rendered OPT scans shown in E-G. Asterisks indicating cavity space. Arrowheads indicating vertically oriented palatal shelves. Arrow indicating an elevated palatal shelf.

Table 1.

The dimensions of the common oral-nasal cavity in wild type and *Has2* cko mutant mice before palatal shelf elevation.

		Embryo number	SB (mm)	NB (mm)	MB (mm)	S-MB (mm)	N-MB (mm)
E13.5	wt	4	1.44±0.20	3.56±0.17	2.08±0.22	0.98±0.07	0.33±0.14
	cko	4	1.46±0.31	3.40±0.36	2.08±0.23	1.02±0.03	0.32±0.19
	cko, %wt		101.6	95.7	100.0	104.1	98.8
	P value		ns	ns	ns	ns	ns
Early	wt	4	1.54±0.12	4.56±0.17	2.94±0.15	1.37±0.11	1.20±0.10
E14.5	cko	4	1.52±0.04	4.18±0.11	2.46±0.04	1.17±0.04	0.69±0.06
	cko, %wt		98.4	91.6	83.6	85.6	57.5
	P value		ns	<0.01	<0.001	<0.05	<0.001

ns, not significant, P>0.05.